Supporting Information

Process Coupling of CO_2 Reduction and 5-HMF Oxidation Mediated by Defect-riched Layered Double Hydroxides

Jingjing Fan[1,#], Yin Zhao[1,#], Qian Wang[1]*, Mingyu Gao[1], Xintao Li[1], Dianqing Li[1,2], Junting Feng[1,2,*]

1 State Key Laboratory of Chemical Resource Engineering, Beijing University of Chemical Technology, 100029, Beijing, China

2 Beijing Engineering Center for Hierarchical Catalysts, Beijing University of Chemical Technology, 100029, Beijing, China

* Corresponding author

wq@mail.buct.edu.cn (Qian Wang); fengjt@mail.buct.edu.cn (Junting Feng)

# These authors contributed equally to this work

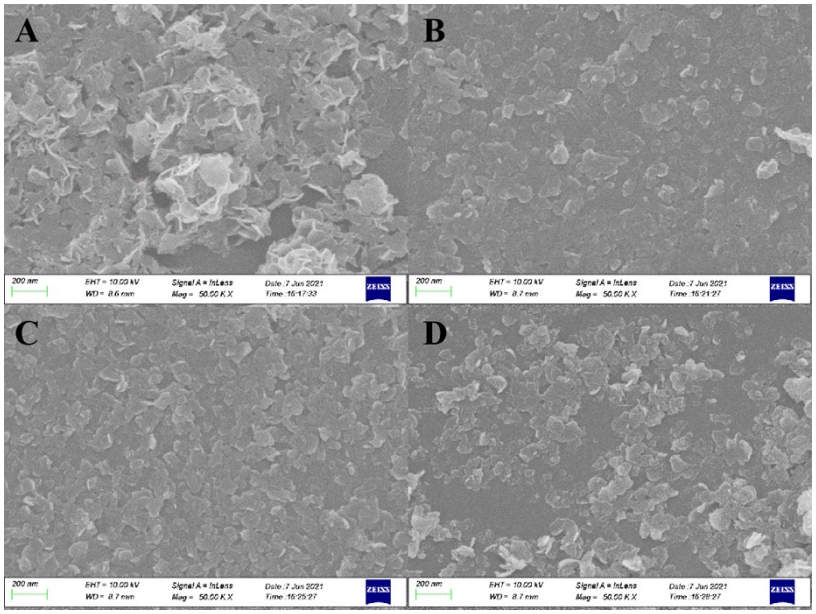

Figure S1 SEM images of the nanoreactors (A) ZnNiFe-LDHs, (B) ZnNiFe-LDHs-E1h, (C) ZnNiFe-LDHs-E2h, (D) ZnNiFe-LDHs-E3h

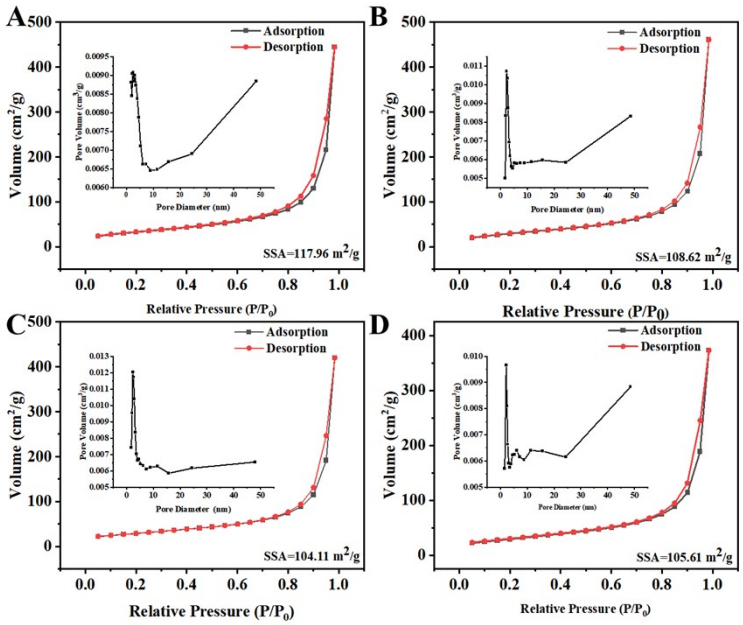

Figure S2. Low temperature N_2 adsorption and desorption curves of nanoreactor before and after etching (A) ZnNiFe-LDHs, (B) ZnNiFe-LDHs-E1h, (C) ZnNiFe-LDHs-E2h, (D) ZnNiFe-LDHs-E3h

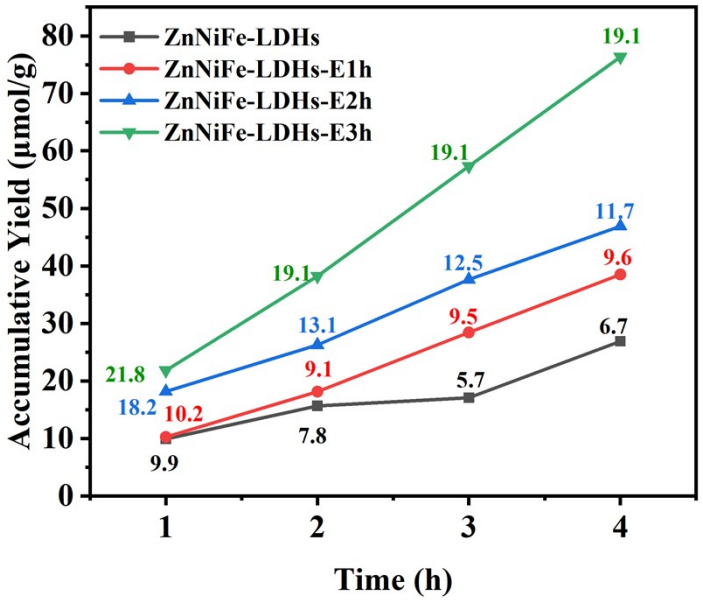

Figure S3. CO time performance plot

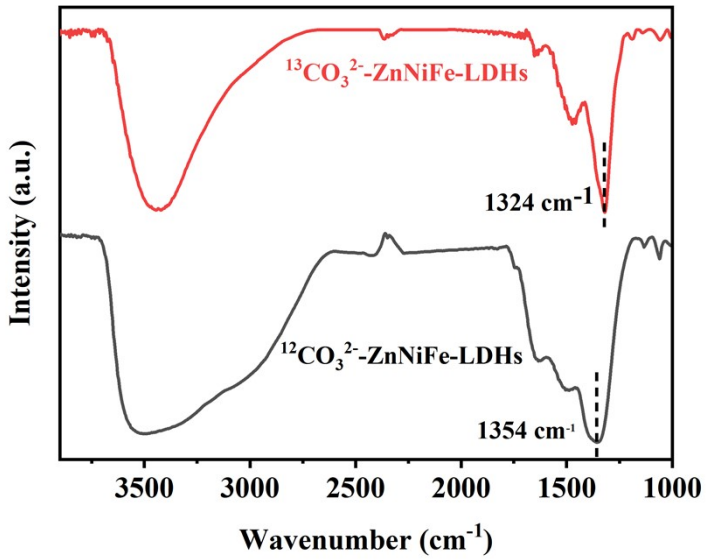

Figure S4. FTIR spectra of different carbon-labeled ZnNiFe-LDHs

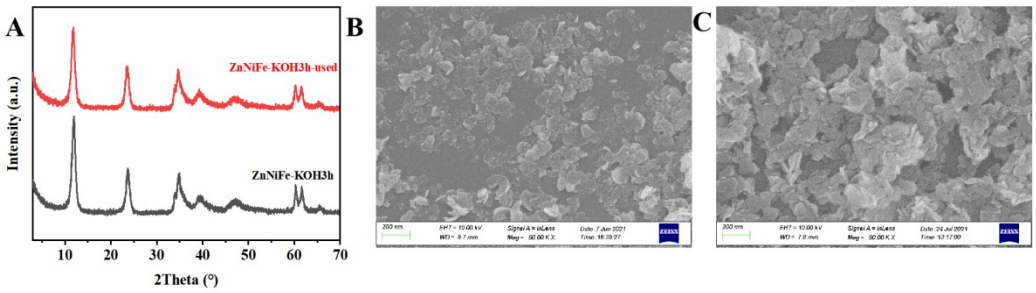

Figure S5. (A) XRD patterns of ZnNiFe-LDHs-E3h before and after the reaction; (B) SEM photo of ZnNiFe-LDHs-E3h before the reaction; (C) SEM photo of ZnNiFe-LDHs-E3h after the reaction

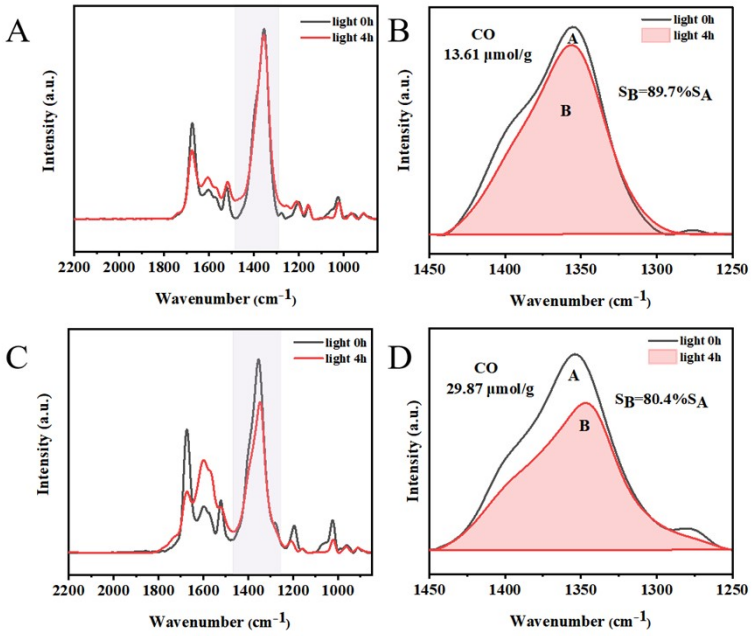

Figure S6. Before and after nanoreactors reaction (A) FTIR spectra of ZnNiFe-LDHs, (B) CO_3^{2-} peak area comparison of ZnNiFe-LDHs, (C) FTIR spectra of ZnNiFe-LDHs-E3h, (D) CO_3^{2-} peak area comparison of ZnNiFe-LDHs-E3h

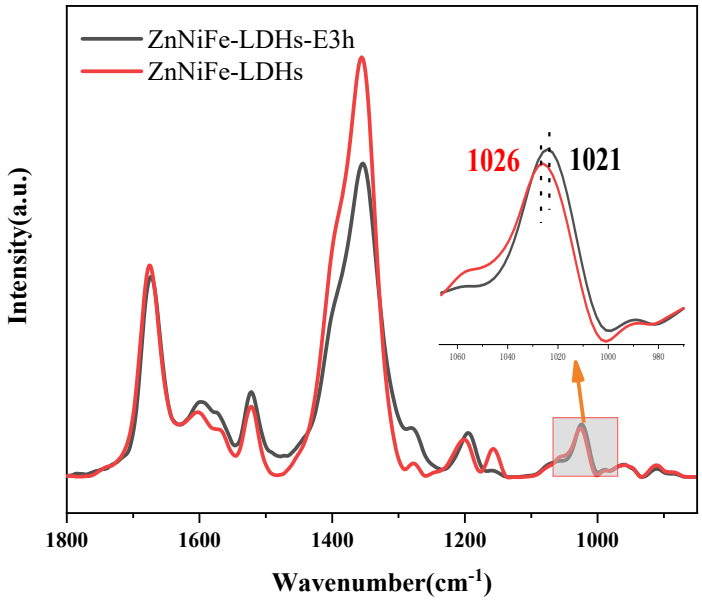

Figure S7. FTIR spectra of 5-HMF adsorbed by the nanoreactor

Table S1. Characteristic structural and size data of the LDHs determined by XRD in solid state

	Peak position[a] (°)		Calculated parameters (nm)				
	003	110	d_{003}[b]	d_{110}[b]	a[c]	c[d]	v[e]
ZnNiFe-LDHs	11.6	59.9	0.76	0.15	0.31	2.29	9.8
ZnNiFe-LDHs-E1h	11.6	60.0	0.76	0.15	0.31	2.29	14.1
ZnNiFe-LDHs-E2h	11.6	60.0	0.76	0.15	0.31	2.29	14.7
ZnNiFe-LDHs-E3h	11.6	60.0	0.76	0.15	0.31	2.29	14.4

a Obtained from the XRD spectra.

b $n\lambda=2d\sin\theta_B$, where n is an integer (in general it is 1), λ is the wavelength of the laser (λ=0.154 nm), d is the lattice spacing and θ_B is the Bragg angle.

c Shortest distance between two cations in the layer and $a=2d_{110}$.

d The width of a unit cell and $c=3d_{003}$.

e $v=K\lambda/\beta\cos\theta_B$, K is the shape factor (0.89 is used in the calculation) and β is the line broadening at the full widths at half maximum in radian obtained by applying Gaussian fits to the peaks.

Table S2. The results of metal content analysis of ZnNiFe-LDHs and ZnNiFe-LDHs-EXh

Nanoreactors	Zn^{2+}（mmol/g）	Ni^{2+}（mmol/g）	Fe^{3+}（mmol/g）	Zn:Ni:Fe	Zn%
ZnNiFe-LDHs	1.00±0.07	3.44±0.10	2.61±0.07	0.38:1.31:1	14.2±0.5
ZnNiFe-LDHs-E1h	0.20±0.02	3.49±0.06	2.51±0.03	0.08:1.39:1	3.2±0.3
ZnNiFe-LDHs-E2h	0.17±0.02	3.48±0.03	2.64±0.02	0.06:1.31:1	2.7±0.3
ZnNiFe-LDHs-E3h	0.10±0.01	3.73±0.02	2.62±0.01	0.04:1.42:1	1.5±0.2

Table S3. Interlayer hydroxyl and carbonate weight loss statistics

Nanoreactors	H_2O（%）	CO_3^{2-}（%）
ZnNiFe-LDHs	15.56	17.03
ZnNiFe-LDHs-E1h	14.70	17.05
ZnNiFe-LDHs-E2h	13.87	17.45
ZnNiFe-LDHs-E3h	11.98	17.00

Table S4. 5-HMF conversion, product selectivity and photogenerated hole/electron ratio

Nanoreactor	5-HMF conversion(%)	Selectivity (%)			Carbon balance(%)	hole/electron
		DFF	FFCA	FDCA		
ZnNiFe-LDHs	8.25	75.41	15.37	7.57	98.35	1.24
ZnNiFe-LDHs-E1h	14.61	68.14	17.76	10.97	96.87	1.32
ZnNiFe-LDHs-E2h	11.59	68.11	20.69	8.55	97.35	1.27
ZnNiFe-LDHs-E3h	24.83	70.73	15.87	8.61	95.21	1.31

Table S5. Comparison of the reaction conditions and performances with other catalysts for photocatalytic CO_2 reduction.

Samples	Light Source	Substrate	Reduced Products ($\mu mol \cdot h^{-1} \cdot g^{-1}$)	Oxidized Product ($\mu mol \cdot h^{-1} \cdot g^{-1}$)	Selectivity (%)	Ref.
CdS/BCN	300 W Xe lamp	CO_2, H_2O/CH_3CN; TEOA	CO: 250	O_2	CO:100	1
One-Unit-Cell $ZnIn_2S_4$	300 W Xe lamp (AM 1.5G)	CO_2, H_2O	CO: 33.2	O_2	CO:100	2
0.5ZIS/TiO_2	300 W Xe lamp	CO_2, H_2O	CO: 23.35 CH_4: 6.19	O_2	CO: 79.0	3
Co-rGO/C_3N_4	300 W Xe lamp ($\lambda >$ 420 nm)	CO_2, H_2O,TEOA, [Ru(bpy)$_3$]$Cl_2 \cdot 6H_2O$	CO: 25	O_2	CO:100	4
CuCoAl-LDHs-E-60	300 W Xe lamp	CO_3^{2-}-LDHs, 5-HMF, CH_3CN	CO:18.3	DFF: 10.4 FFCA: 5.5 FDCA:1.7	CO:>99.0 DFF: 59.1	5
Pt/MgFe-LDHs-15%	300 W Xe lamp	CO_3^{2-}-LDHs, glycerol	CO: 15.8 CH_4: 43.6 H_2:26.9	DHA: 147.5 LA: 128.2	CO: 26.6 CH_4: 73.4 DHA: 53.5 LA: 46.5	6
ZnNiFe-	**300 W Xe**	**CO_3^{2-}-**	**CO: 19.1**	**DFF: 13.8**	**CO: >99.0**	**This**

LDHs-E3h	**lamp**	**LDHs, 5-HMF, CH_3CN**	**FFCA: 3.1 FDCA:1.7**	**DFF: 74.3**	**Work**

References：

(1) Zhou, M.; Wang, S.; Yang, P.; Huang, C.; Wang, X. Boron Carbon Nitride Semiconductors Decorated with CdS Nanoparticles for Photocatalytic Reduction of CO2. *ACS Catalysis* **2018**, *8* (6), 4928-4936.

(2) Jiao, X.; Chen, Z.; Li, X.; Sun, Y.; Gao, S.; Yan, W.; Wang, C.; Zhang, Q.; Lin, Y.; Luo, Y.; et al. Defect-Mediated Electron–Hole Separation in One-Unit-Cell ZnIn2S4 Layers for Boosted Solar-Driven CO2 Reduction. *Journal of the American Chemical Society* **2017**, *139* (22), 7586-7594.

(3) She, H.; Wang, Y.; Zhou, H.; Li, Y.; Wang, L.; Huang, J.; Wang, Q. Preparation of Zn3In2S6/TiO2 for Enhanced CO2 Photocatalytic Reduction Activity Via Z-scheme Electron Transfer. *ChemCatChem* **2019**, *11* (2), 753-759.

(4) Jiang, J.; Duan, D.; Ma, J.; Jiang, Y.; Long, R.; Gao, C.; Xiong, Y. Van der waals heterostructures by single cobalt sites-anchored graphene and g-C3N4 nanosheets for photocatalytic syngas production with tunable CO/H2 ratio. *Applied Catalysis B: Environmental* **2021**, *295*, 120261.

(51) Fan, J.; Yue, X.; Liu, Y.; Li, D.; Feng, J. An integration system derived from LDHs for CO2 direct capture and photocatalytic coupling reaction. *Chem Catalysis* **2022**, *2* (3), 531-549.

(6) Gao, M.; Fan, J.; Fan, J.; Wang, Q.; Li, D.; Feng, J. Process coupling of CO2 and glycerol comprehensive utilization based on anionic 2D nanomaterial. *AIChE Journal* **2022**, e17976.